Pion scattering from C and Ca at 800 MeV/c

D. Marlow, P. D. Barnes, N. J. Colella, S. A. Dytman,* R. A. Eisenstein,† R. Grace, P. Pile,‡
F. Takeutchi,§ and W. R. Wharton
Carnegie-Mellon University, Pittsburgh, Pennsylvania 15213

S. Bart, D. Hancock, R. Hackenberg, E. Hungerford, W. Mayes, L. Pinsky, and T. Williams**
University of Houston, Houston, Texas 77004

R. Chrien, H. Palevsky, and R. Sutter
Brookhaven National Laboratory, Upton, New York 11973
(Received 15 May 1984)

Results from $\pi^{\pm}$ elastic and inelastic scattering from ^{12}C and ^{40}Ca are reported. The data were all taken at an incident momentum of 800 MeV/c over an angular range from 4° to 38°. The elastic data are compared to first-order optical model calculations in momentum space; qualitative agreement is obtained. The inelastic data (from ^{12}C only) are compared to distorted-wave Born approximation calculations, and reasonable agreement is found if realistic inelastic transition densities are used.

I. INTRODUCTION

The interaction of pions with nuclei has been actively studied for about ten years.[1-3] The main focus of this effort to date has been to work at energies at or below the pion production threshold, which occurs for the πN interaction at π kinetic energies of $\sim$175 MeV. At these energies the basic πN interaction is completely elastic and determined by rather few partial waves, the dominant one being the P_{33}, which has a strong resonance (the Δ) at $\sqrt{s}=1232$ MeV. This resonance is the only one occurring below 1440 MeV. For the purpose of testing multiple scattering formulations of elastic π scattering, it has been very important to make use of the dramatic change of the πN amplitude with energy.[1-3]

In the work reported here, we present the first precise measurements of elastic and inelastic π scattering at an energy substantially above the π production threshold. At this energy, the $\Delta(1232)$ resonance is no longer dominant, and a number of other N* and Δ resonances are expected to play an important role (see Fig. 1). We are thus examining π-nucleus scattering under substantially different dynamical conditions than have previous experiments. From the point of view of nuclear structure studies, scattering at these energies produces rather large momentum transfers even at small scattering angles. It may therefore be possible to give an accurate treatment of the process using an eikonal approximation for the pion waves and a single scattering impulse approximation for the π-nucleus interaction. The physics interest in performing nuclear scattering measurements at these energies is summarized in Ref. 4. To date, very few calculations for this energy range have been made.[5-7].

In Sec. II we describe the main features of the apparatus and the experiment. These are almost identical to what was reported earlier[8,9] for our kaon scattering measurement. In Sec. III, we briefly describe the basic πN and π-nucleus interactions, and compare our data to some first-order optical potential calculations. In Sec. IV we draw some conclusions from the work.

II. EXPERIMENTAL PROCEDURE

The pion scattering measurements were performed simultaneously with kaon scattering measurements[8,9] using the low energy separated beam (LESB-I) at the

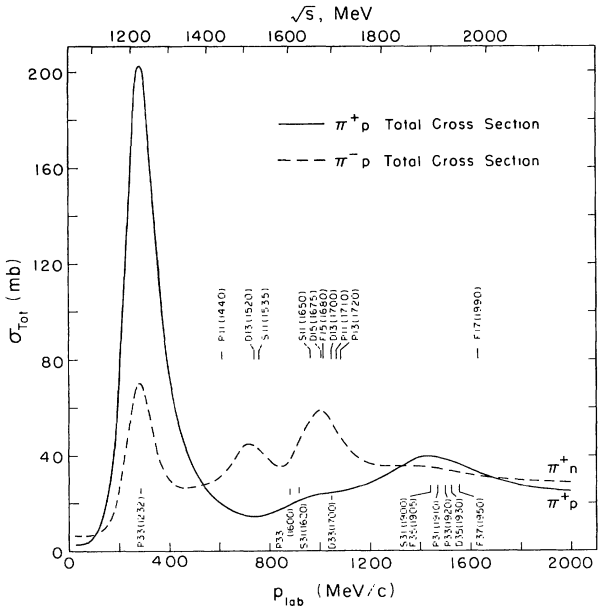

FIG. 1. Total π^+p and π^+n cross sections plotted against the lab π momentum (p_{lab}) and total center of mass energy $\sqrt{s}$. The positions of several prominent N* and Δ resonances are shown.

Brookhaven National Laboratory alternating gradient synchrotron (AGS). A detailed description of the experimental apparatus and the data collection and reduction procedures is contained in Refs. 8 and 9. Only a brief description of the experimental procedure will be given here.

A. The pion beam and spectrometers

The LESB-I beam line was designed to deliver beams of kaons and antiprotons which have a substantial fraction of unwanted particles separated out by means of an E-cross-B velocity filter. However, even with the filter tuned to pass only 800 MeV/c kaons, the ratio of unwanted particles (mostly pions and muons) to kaons was about 12:1. The pion flux on the target was then larger than the kaon flux. The pion-plus-muon part of the beam was easily separated from the kaon part by measuring the time-of-flight between two scintillators; however, the pion and muon components remained unresolved in time.

A schematic of the LESB-I beam line and the momentum loss spectrometer system as it was configured during the experiment is shown in Fig. 2. The incident beam momentum was measured using spectrometer 1 and the scattered momentum was measured with spectrometer 2. The particle type was determined by its time-of-flight between scintillators S1 and ST for the incident beam, and ST and S2 for the scattered beam. Multiwire proportional chambers $P1$ through $P6$ were used to measure the particle trajectories for momentum and scattering angle determination as well as vertex reconstruction at the target. The detector labeled CK in Fig. 2 was a lucite Čerenkov counter designed to detect particles with a speed of about 0.85c, which occurs for an 800 MeV/c kaon. The beam transport chambers of LESB-I and the spectrometers were evacuated; however, the production target, mass slit area, detector areas, and experimental target areas were located in air. Spectrometer 2 could be rotated to 30 deg, and had about a 12 msr solid angle and a 5% momentum acceptance. The overall system resolution was 2 to 2.5 MeV depending on the target thickness.

B. Data collection and reduction

Simultaneously with the logging of kaon scattering data, pion beam events (defined by $S1 \cdot ST \cdot \bar{C}_K$) and pion scattering events ($S1 \cdot ST \cdot S2 \cdot \bar{C}_K$) were recorded on magnetic tape. The scattered pion events were prescaled by factors ranging typically from 2 to 10, depending upon the even rates. The prescale factors were chosen so that the system dead time was not dominated by pion scattering events. The accepted pion flux was therefore comparable to the kaon flux. The typical pion-plus-muon flux at the target was 3×10^5 per 1 sec beam spill, while the kaon flux was an order of magnitude less. The pion beam events were prescaled typically by a factor 2×10^5, so that one or two events were recorded per beam spill. The beam events were used to determine the spectrometer efficiency and provided input for a Monte Carlo program[8,9] that predicted the solid angle of the second spectrometer as a function of scattering angle. This permitted an initial estimate of the absolute cross section scale. This was subsequently modified by normalization to pion-hydrogen scattering data (see the following).

The pion data reduction process paralleled that of the kaon data reduction described in Refs. 8 and 9. Briefly, the following software cuts were applied to the data:

1. A multiplicity of one was required in chambers P_1, P_2, and P_3.
2. The event vertex was required to lie with the target volume.
3. The times-of-flight between S1 and ST and between ST and S2 were required to lie within well-defined windows.
4. An incident pion was required to have momentum within $\pm2.5\%$ of the central value (800 MeV/c).

The cuts that involved only parameters measured by the pion beam spectrometer were also applied to the pion beam set of data in order to remove any systematic errors resulting from cuts that were too stringent. The data were summed together for all spectrometer settings and divided into 1 deg scattering angle bins, corresponding to the overall system angular resolution of about 1 deg FWHM.

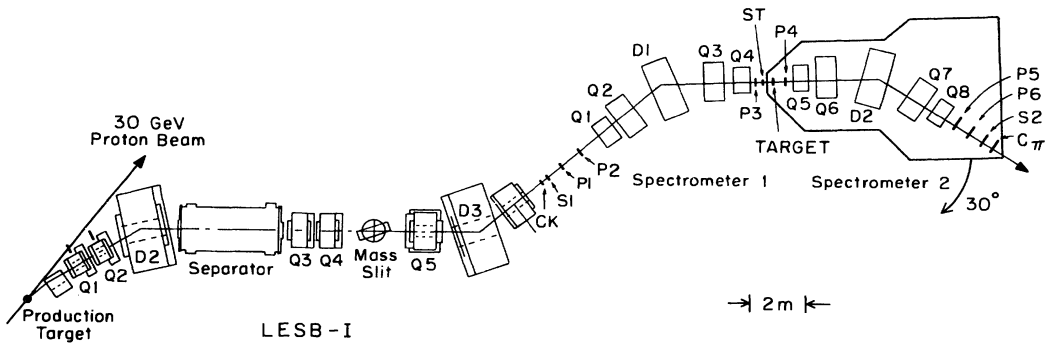

FIG. 2. The BNL AGS LESB-I beam line and spectrometer system as it was configured during this experiment.

Peak areas in all spectra were determined by fitting Gaussian shapes (of variable height but fixed width) located at the known positions of prominent peaks. Spectra for the natural carbon and calcium targets are shown in Figs. 3(a) and (b), respectively. Because of the large background under the excited states in the calcium data, only the elastic data were analyzed for this nucleus. In the carbon case, the background under the inelastic peaks was estimated at each angle by using an adjustable linear function. It was not possible to obtain reliable cross sections at angles smaller than 14.4 deg (see Tables I and II). The errors quoted for these data include the uncertainty due to fitting.

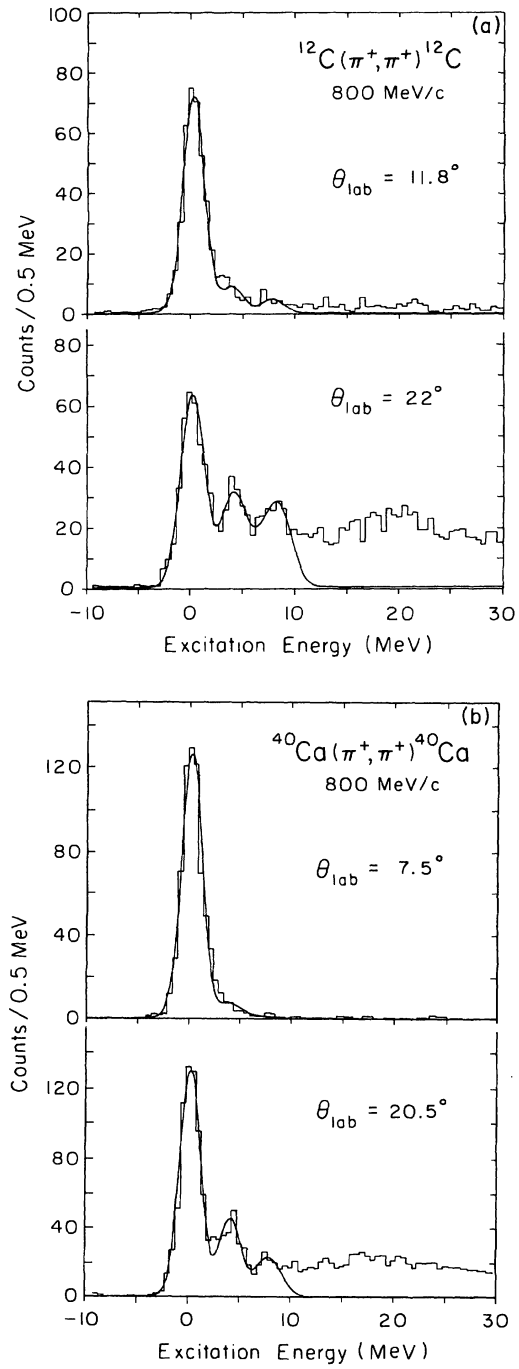

FIG. 3. Representative C and Ca spectra for two different scattering angles. The solid lines are fits to π^+ data. Data shown are for selected one-degree angle bins.

C. Absolute normalization of differential cross sections

The overall normalization of the differential cross sections was based on pion scattering from protons. The data were taken over a limited angular range using a 1.7 g/cm^2 CH_2 target. The analysis cuts applied to the proton data were identical to those applied to the carbon and calcium data. Figures 4(a) and (b) show both the positive and negative pion scattering differential cross section data multiplied by factors of 2.3 and 2.1, respectively, in order to normalize the data to the dashed lines. The dashed lines represent linear interpolations of theoretical πN

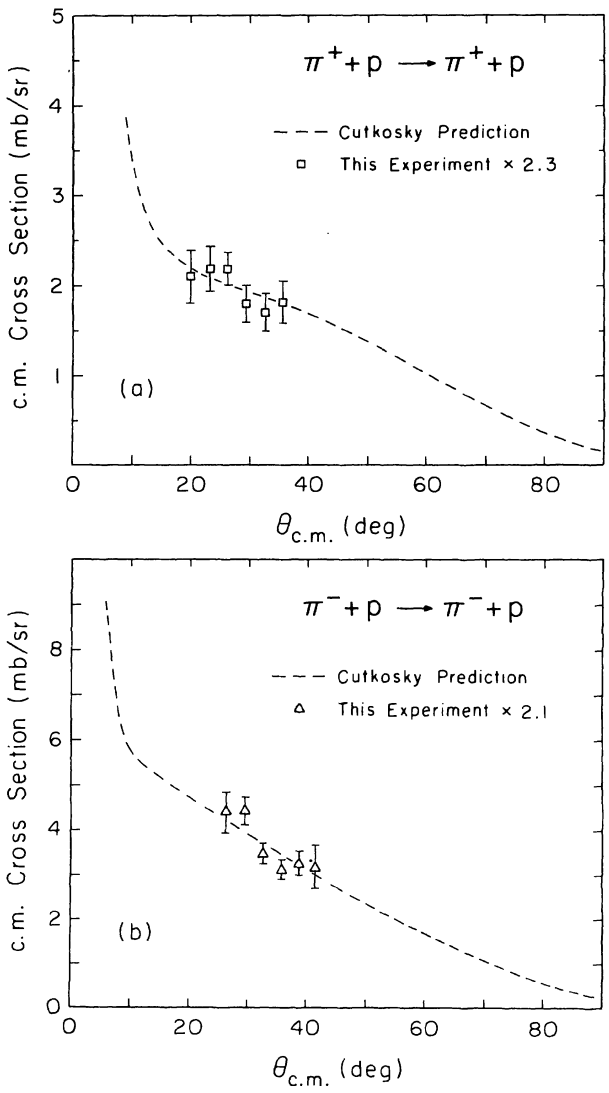

FIG. 4. Comparison of p(π,π)p data from this experiment to cross sections generated from the phase shift set of Cutkosky *et al.* (Ref. 10).

cross sections obtained using the phase shift set of Cutkosky *et al.*[10] The Cutkosky πN amplitudes contain 80 partial waves and were based on an amalgamated data set[11] which includes incident pion momenta between 420 and 2000 MeV/c. To obtain the amplitudes for 800 MeV/c, a linear interpolation was made using the Cutkosky results from 770 and 820 MeV/c. The same normalizing factors used for the proton data were then applied to both the carbon and calcium sets of data. The normalization factors are accurate to about $\pm 5\%$ relative to the interpolated lines; however, the uncertainty in the absolute magnitude of the amalgamated differential cross section data is about $\pm 15\%$ for both the positive and negative pion data.

The large factors needed to normalize the data indicate that the muon component of the incident beam was larger than the pion component. The 1 nsec FWHM time-of-flight resolution between S1 and S2 was not adequate to resolve the 350 psec pion-muon flight time difference. During the tuning phases of a recent experiment using a negative 720 MeV/c kaon beam at the same beam line, a time-of-flight measurement was made between S1 and a small scintillator located just after S2. Figure 5 shows the

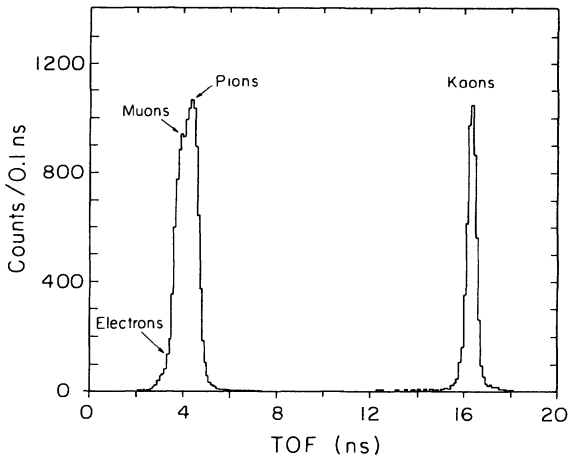

FIG. 5. Time-of-flight spectrum for 720 MeV/c particles over a 17.6 m flight path. The resolution was about 400 psec FWHM (see the text).

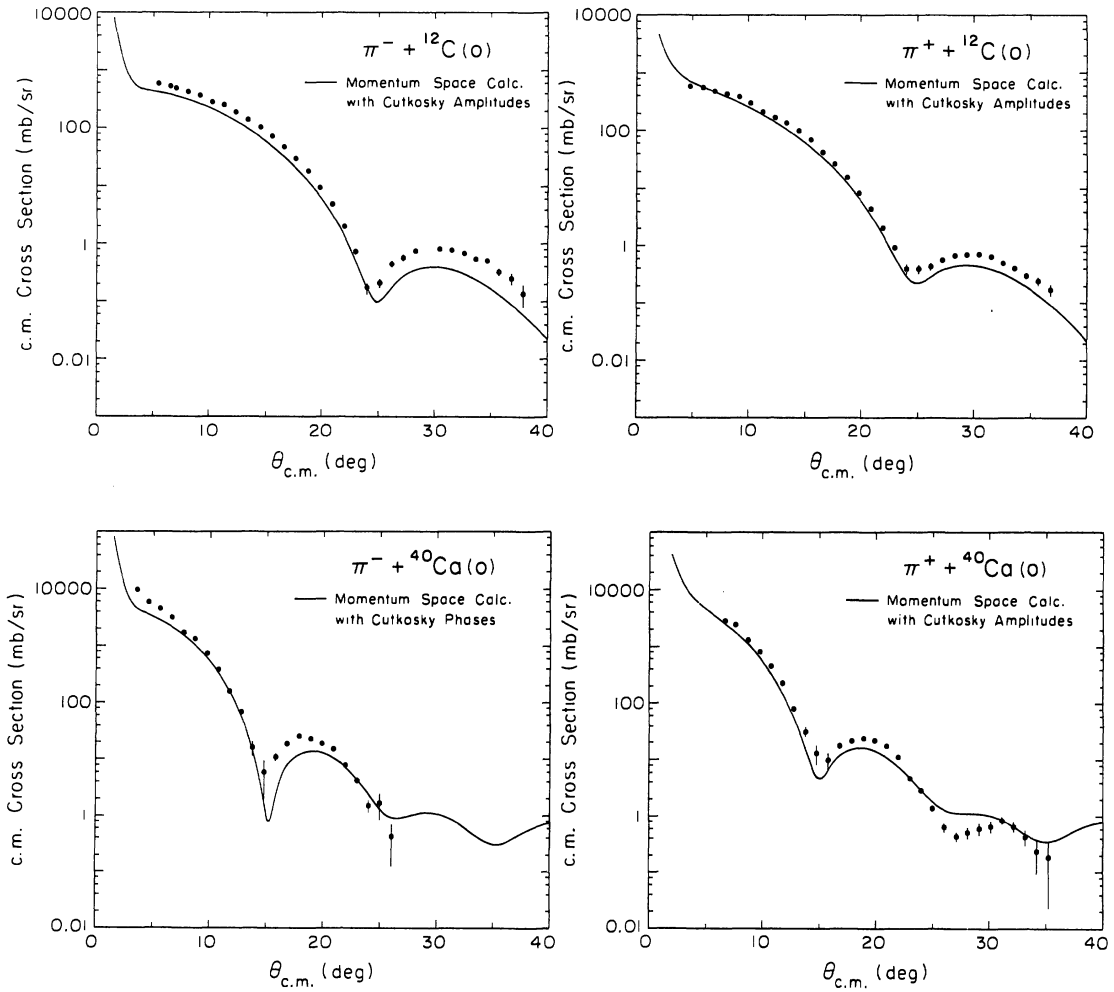

FIG. 6. Comparison of the elastic data taken in this experiment to calculations using KPIT (Ref. 12) and Cutkosky πN amplitudes (Ref. 10). See the text.

results of this test along with the expected positions of the pion, muon, and electron peaks relative to the kaon peak. The broadening of the pion peak is due to about an equal number of pions and muons and a relatively small number of electrons. The relative number of pions and muons in the beam is dependent upon the beam momentum, beam polarity, and the actual tune of the elements in the beam line. Therefore, the pion to muon ratio that would be predicted by a fit to the data of Fig. 5 could not be used to predict the ratio as it was during the running of the pion scattering experiment. The data contained in Fig. 5 do, however, support the large normalization factor needed to bring the present data into agreement with previous absolute cross section measurements, parametrized here by the Cutkosky amplitudes.[10]

For the carbon target the beam energy at the target center was approximately 673.2 MeV, while for the calcium target it was 674.2 MeV. Cross sections for all of the states observed in our experiment are given in Tables I–III.

III. INTERPRETATION

Figure 6 shows all of the elastic data accumulated in this experiment. The angular range extends from about 4° to about 38°, and was limited by the physical constraints of the spectrometer system and the parasitic nature of this measurement. The angular distributions for both nuclei fall rather steeply with angle and display minima which are characteristic of the nuclear sizes involved. The minima for the π^- data are perhaps slightly sharper than for the π^+ data; otherwise the data sets are very similar in overall magnitude of cross section and position of the minima. This situation is different than for the kaon data collected[8] at the same incident momentum. In that case, the K^+ minima were shifted to larger angles (by $\sim 3°$ typically) than those for K^-, possibly indicating that the K^+ projectile sees a smaller nucleus than does the K^-.

In a simple first-order factorized optical potential description, these differences would be attributed to the behavior of the basic πN and KN amplitudes. In the kaon case, the K^-N amplitude is somewhat larger than K^+N, and furthermore, contains several resonances in the region of interest. The K^+N system in this region contains no known resonances. In the pion case, the π^+N and π^-N amplitudes are related to each other via isospin invariance since the π^+ and π^- are members of the same isospin multiplet. To first approximation, π^+ and π^- scattering from self-conjugate nuclei ought to be very

TABLE I. Our measured cross sections for π^- scattering from ^{12}C at 800 MeV/c. The overall normalization uncertainty is ±15%; the errors listed are statistical only.

c.m. angle (deg)	Elastic c.m. cross section (mb/sr)	Error	2^+ (4.4 MeV) c.m. cross section (mb/sr)	Error	3^- (9.6 MeV) c.m. cross section (mb/sr)	Error
5.38	587	59.1				
6.45	526	34.3				
6.96	500	26.7				
8.03	423	19.1				
9.10	364	14.5				
10.2	278	9.92				
11.2	252	7.44				
12.3	191	4.96				
13.4	137	3.43				
14.4	102	2.48	16.41	1.80		
15.5	72.6	1.91	16.35	1.51		
16.6	47.7	1.14	14.55	1.22	7.01	0.84
17.6	29.6	0.953	13.10	1.01	6.30	0.71
18.7	18.0	0.591	11.15	0.76	6.23	0.61
19.8	9.63	0.362	9.93	0.76	5.33	0.50
20.8	4.94	0.229	8.19	0.57	5.21	0.44
21.9	2.02	0.143	6.40	0.38	4.30	0.36
23.0	0.725	0.0782	5.23	0.38	3.71	0.31
24.0	0.174	0.0419	3.76	0.29	2.90	0.25
25.1	0.214	0.0439	3.02	0.23	2.52	0.21
26.2	0.444	0.0572	2.10	0.19	1.83	0.17
27.2	0.570	0.0610	1.43	0.15	1.30	0.13
28.3	0.751	0.0667	0.993	0.11	1.07	0.13
30.4	0.814	0.0648	0.420	0.076	0.592	0.096
31.5	0.793	0.0648	0.248	0.057	0.420	0.076
32.5	0.702	0.0667	0.229	0.076	0.340	0.076
33.6	0.543	0.0648	0.174	0.063	0.214	0.076
34.7	0.507	0.0610	0.107	0.050	0.113	0.057
35.7	0.332	0.0534	0.080	0.046		
36.8	0.250	0.0572				
37.8	0.139	0.0591				

similar. This expectation seems to be borne out; see Fig. 6. In addition, when the π^+ and π^- data sets from a given nucleus are overlaid, they agree very well with each other.

A. Momentum space calculations

Figure 6 shows calculations done in momentum space to be compared to the data. The calculations presented here were done with the computer code KPIT,[12] which uses a first-order factorized "$t\rho$" optical potential treatment, and includes a finite πN range, a reasonable off-shell extrapolation, and exact handling of all partial waves in the πN elementary t matrix. From a technical point of view, KPIT thus offers a better treatment than conventional coordinate space calculations.

The elementary πN amplitudes at 800 MeV/c were obtained by linear interpolation from the amplitudes given by Cutkosky *et al.*[10] The range parameter used in the Yukawa off-shell form factor was 800 MeV/c; the exact value of this number had only a slight effect on the calculation. The nucleon finite size was factored out of the nuclear density by using the techniques of Ref. 13 and a nucleon form factor given by

$$\rho_{\text{nucl}}(q)=(1+q^2/q_0^2)^{-2}\ ,$$

with q_0 taken as 4.26 fm^{-1} (see Ref. 14).

It is interesting that all of the momentum space calculations persistently underestimate the data; the situation is most severe for the ^{12}C results. The reason for this is not understood at present.

Indeed, one of the hopes for π-nucleus scattering in this energy range was that simple treatments of the elastic process would suffice. Born approximation calculations for these nuclei are in fact not much different than the full KPIT calculation which uses the "$t\rho$" optical potential. Apparently, bringing the calculation into agreement with the data will require a more detailed optical potential treatment.

Some evidence supporting this statement can be seen in Table V, where the parameters of a best-fit Kisslinger optical potential are presented. It is seen that the adjusted parameters are quite different from the free πN values quoted; in particular, the data seem to require a strongly repulsive π-nucleus s-wave term. The geometrical parameters of the potential were held fixed in making these fits. These results were used in making the inelastic calculations described in the following.

TABLE II. Our measured cross sections for π^+ scattering from ^{12}C at 800 MeV/c. See Table I.

c.m. angle (deg)	Elastic c.m. cross section (mb/sr)	Error	2^+ (4.4 MeV) c.m. cross section (mb/sr)	Error	3^- (9.6 MeV) c.m. cross section (mb/sr)	Error
4.81	579	60.6				
5.89	560	37.6				
6.96	481	25.1				
8.03	424	18.6				
9.10	378	15.0				
10.2	299	10.7				
11.2	208	6.27				
12.3	166	4.39				
13.4	133	3.13				
14.4	95.9	2.30	16.72	1.88		
15.5	67.9	1.71	14.63	1.46		
16.6	42.0	1.21	13.00	1.21	6.29	0.84
17.6	26.3	0.815	10.3	0.92	5.08	0.65
18.7	15.4	0.585	9.45	0.79	5.18	0.59
19.8	8.17	0.376	7.96	0.63	4.45	0.46
20.8	4.41	0.272	6.44	0.50	3.93	0.40
21.9	2.05	0.173	5.25	0.42	3.74	0.36
23.0	0.919	0.115	4.43	0.36	3.30	0.31
24.0	0.397	0.0794	3.65	0.27	2.70	0.25
25.1	0.397	0.0731	2.63	0.23	2.19	0.21
26.2	0.439	0.0690	1.90	0.17	1.69	0.17
27.2	0.564	0.0606	1.44	0.15	1.34	0.15
28.3	0.690	0.0669	1.00	0.13	0.886	0.109
29.4	0.711	0.0627	0.627	0.084	0.752	0.096
30.4	0.711	0.0543	0.418	0.063	0.556	0.084
31.5	0.648	0.0522	0.230	0.063	0.435	0.073
32.5	0.502	0.0439	0.123	0.040	0.284	0.061
33.6	0.403	0.0418	0.105	0.040	0.224	0.056
34.7	0.299	0.0418	0.117	0.046	0.130	0.048
35.7	0.244	0.0481	0.0711	0.040		
36.8	0.171	0.0460				

TABLE III. Our measured cross sections for π^+ scattering from ^{40}Ca at 800 MeV/c. See Table I.

c.m. angle (deg)	π^- c.m. cross section (mb/sr)	Error	π^+ c.m. cross section (mb/sr)	Error
3.58	9720	651		
4.60	5830	321		
5.62	4450	194		
6.64	3110	125	2750	124
7.66	1710	67.3	2420	97.7
8.68	1290	45.5	1280	47.7
9.71	711	29.7	809	34.7
10.72	380	17.2	445	26.0
11.75	157	9.70	230	21.7
12.77	67.7	5.35	79.4	9.98
13.79	15.9	4.75	32.1	7.38
14.81	5.92	4.16	13.6	5.43
15.82	11.0	1.86	10.2	3.49
16.85	18.8	1.66	17.8	2.43
17.87	25.3	1.58	21.6	1.65
18.89	23.2	1.19	24.0	1.28
19.91	19.3	1.11	21.7	0.977
20.93	15.3	0.950	17.6	0.760
21.95	7.90	0.713	11.2	0.543
22.97	4.28	0.515	4.86	0.369
23.99	1.52	0.436	2.91	0.260
25.01	1.68	0.851	1.40	0.178
26.03	0.416	0.297	0.638	0.124
27.05			0.436	0.0998
28.07			0.510	0.130
29.09			0.605	0.171
30.11			0.658	0.182
31.13			0.846	0.156
32.15			0.660	0.156
33.16			0.430	0.148
34.18			0.232	0.143
35.20			0.191	0.169

TABLE IV. Geometrical parameters of the nuclei studied in the experiment. The ^{12}C density is the modified harmonic oscillator and ^{40}C is the three-parameter Fermi (see Ref. 18). The rows labeled "charge density" are unchanged electron scattering values while the "point density" values result after making a correction for nucleon size.

		c	a	
^{12}C	Charge density	1.649	1.247	
	Point density	1.51	2.33	
		c	z	w
^{40}Ca	Charge density	3.766	0.586	−0.164
	Point density	3.671	0.507	−0.065

TABLE V. Table of optical model parameters b_0 and b_1 obtained using πN amplitudes of Ref. 10, and also from a best fit procedure. Since Fermi averaging is not included, b_0 and b_1 will each remain constant for π^+ or π^- and for ^{12}C and ^{40}Ca. Set A: b_0 includes only s-wave information; b_1 includes only p wave. Set B: b_0 includes s waves and $l=2$–$l=4$ waves; b_1 is unchanged. Set C: b_0 includes all partial waves $l=0$–$l=4$. Best fits used the point geometry of Table IV.

	Re(b_0)	Im(b_0)	Re(b_1)	Im(b_1)
A	−0.14	0.21	−0.44	0.32
B	0.13	0.66	−0.44	0.32
C	−0.31	0.98		
Best fit, π^+-^{12}C	−1.47±0.15	−0.13±0.23	1.46±0.18	0.91±0.24
Best fit, π^--^{12}C	−1.03±0.30	0.25±0.46	0.73±0.35	0.57±0.46

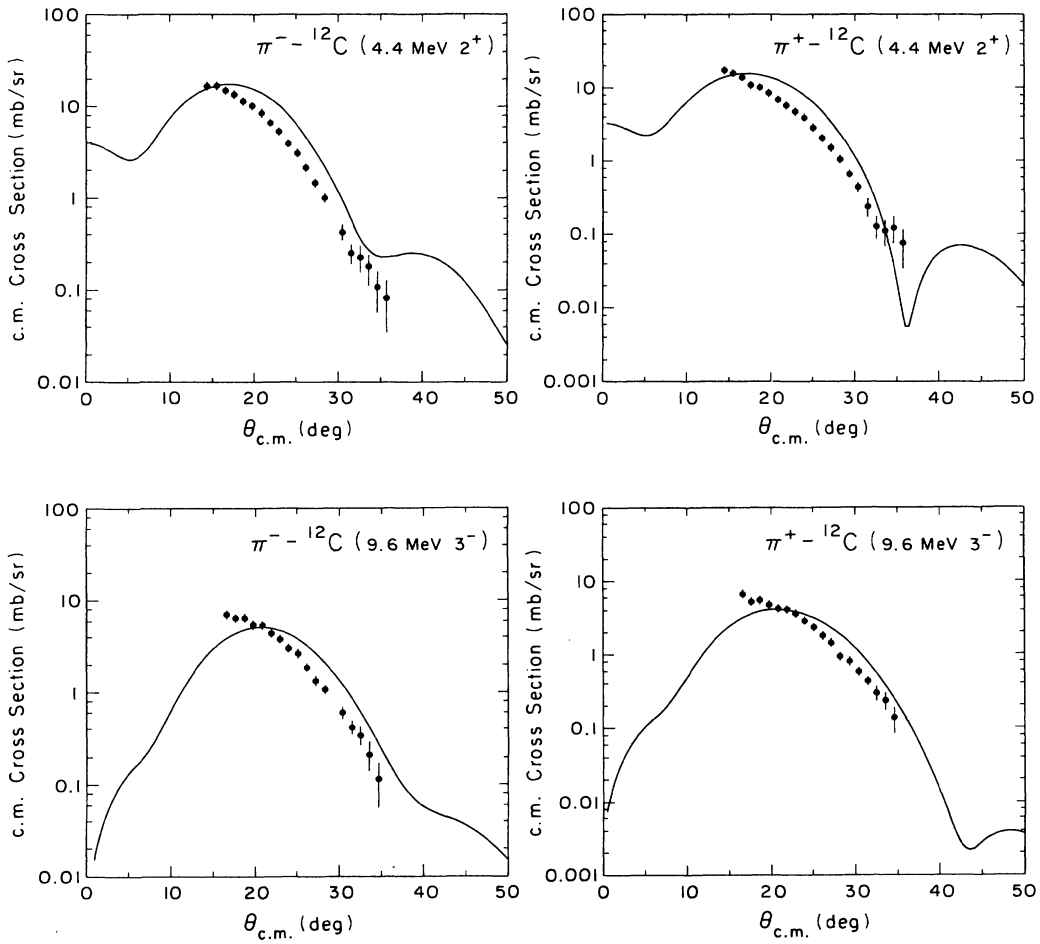

FIG. 7. Comparison of the inelastic data taken in this experiment to DWBA calculations made with NDWPI (Ref. 16). The curves are obtained using a phenomenological electron scattering transition density (Ref. 17) and a best-fit optical potential for the elastic channel. See the text.

B. Inelastic scattering calculations

Data were also accumulated for the inelastic scattering of pions to the 2^+ and 3^- states in ^{12}C at 4.4 and 9.6 MeV (see Tables I and II). These states have been studied previously with inelastic pion scattering in the Δ region by Morris *et al.*[15] The data from our experiment are shown in Fig. 7 compared to calculations using the coordinate space distorted wave code NDWPI.[16] The inelastic transitions are described using phenomenological transition densities which are taken from fits to inelastic electron scattering, as presented by Gustaffson and Lambert.[17] These densities are of the form

$$\rho_{\rm tr}^{L}(r)=r^{L}(a+br^2)e^{-dr^2},$$

with the parameters a, b, and d depending on the transition involved. For the 2^+ state, $a=0.0191$, $b=0.0093$, and $d=0.437$. For the 3^- state, $a=0.0094$, $b=0.0$, and $d=0.325$. The elastic channel was described phenomenologically by a best-fit optical potential of the Kisslinger form (see Ref. 16); the geometrical parameters used are given in Table IV (see Ref. 18) and the adjusted optical model parameters in Table V. The data appear to be well described by this prescription; attempts to fit the data using unadjusted elastic optical potentials or other transition densities (i.e., Gillet-Vinh-Mau particle-hole calculations[19] or collective models[16]) gave poorer results, as expected.

IV. CONCLUSIONS

Pion elastic and inelastic scattering data at 800 MeV/c on targets of ^{12}C and ^{40}Ca have been taken at the BNL Moby Dick spectrometer facility. The π^+ and π^- elastic scattering data from each of these self-conjugate nuclei are essentially identical in magnitude and position of the minima. This feature, which is due to isospin invariance, is expected. It is interesting to compare these data to the $K^{\pm}$ data[8] taken at the same momentum, for which systematic $K^{\pm}$ differences were observed.

Momentum space calculations (with no adjustable parameters) have been performed for our pion elastic

scattering data. While reasonable qualitative agreement with the data is obtained, the calculations are systematically low, even in the forward angle region. The reasons for this are not understood. This possibly indicates the need for better first-order calculations, perhaps using nonfactorized optical potentials and other improvements. The input πN amplitudes are well known and are not likely to be the source of difficulty.

The inelastic data on carbon are reasonably well described using a coordinate space distorted-wave calculation. In order to describe the elastic channel, point nucleon matter distributions were used in a Kisslinger potential with adjustable parameters. Good fits to the elastic data were obtained. The inelastic transition form factors were taken from electron scattering.

ACKNOWLEDGMENTS

We would like to thank the staff of the Brookhaven AGS facility and also members of the BNL Physics Department for their considerable help in mounting and executing the experiment. Dr. M. May, one of the designers of Moby Dick, provided useful information about its operation. We would also like to mention Bill Espensen, Vito Manzella, and Al Minn. Professor R. Cutkosky of Carnegie-Mellon University kindly provided the πN amplitudes used in our calculations. We appreciate also the interest shown in this project by Dr. James A. Carr and Professor Joseph Chalmers. This work was supported by the U.S. D.O.E.

---

*Present address: Physics Department, University of Pittsburgh, Pittsburgh, PA 15260.

†Present address: Nuclear Physics Laboratory, University of Illinois, Champaign, IL 61820.

‡Present address: Brookhaven National Laboratory, Upton, NY 11973.

§Present address: Physics Department, Kyoto Sangyo University, Kyoto 603, Japan.

**Present address: Texaco Research Labs, Houston, TX 77005.

[1]C. H. Q. Ingram, in Proceedings of the Ninth International Conference on High Energy Physics and Nuclear Structure, edited by P. Catillon, P. Radvanyi, and M. Porneuf (North-Holland, Amsterdam, 1982).

[2]R. A. Eisenstein, in Proceedings of the Workshop on Nuclear and Particle Physics at Energies up to 31 GeV: New and Future Aspects, edited by J. D. Bowman, L. S. Kisslinger, and R. R. Silbar, Los Alamos National Laboratory Report LA-8775-C, 1981.

[3]R. H. Landau, in *Proceedings of the Eighth International Conference on High Energy Physics and Nuclear Structure,* edited by D. F. Measday and A. W. Thomas (North-Holland, Amsterdam, 1979).

[4]H. A. Thiessen, see Ref. 2.

[5]Alan K. Dozier and Joseph S. Chalmers, Phys. Rev. C **23**, 399 (1981).

[6]Alan K. Dozier and Joseph S. Chalmers, Phys. Rec. C **23**, 563 (1981).

[7]M. M. Sternheim, Phys. Rev. C **24**, 1812 (1981).

[8]D. Marlow, P. D. Barnes, N. J. Colella, S. A. Dytman, R. A. Eisenstein, R. Grace, F. Takeutchi, W. R. Wharton, S. Bart, D. Hancock, R. Hackenberg, E. Hungerford, W. Mayes, L. Pinsky, T. Williams, R. Chrien, H. Palevsky, and R. Sutter, Phys. Rev. C **25**, 2619 (1982).

[9]D. R. Marlow, Ph.D. thesis, Carnegie-Mellon University, 1981 (unpublished).

[10]R. E. Cutkosky, R. E. Hendrick, J. W. Alcock, Y. A. Chao, R. G. Lipes, and J. C. Sandusky, Phys. Rev. D **20**, 2804 (1979); R. E. Cutkosky, private communication.

[11]R. L. Kelly and R. E. Cutkosky, Phys. Rev. D **20**, 2782 (1979).

[12]R. A. Eisenstein and F. Tabakin, Comput. Phys. Commun. **12**, 237 (1976).

[13]R. A. Eisenstein and F. Tabakin, Phys. Rev. C **26**, 1 (1982).

[14]W. S. C. Williams, *An Introduction to Elementary Particles* (Academic, New York, 1971), p. 451.

[15]C. L. Morris, K. T. Boyer, C. F. Moore, C. J. Harvey, K. J. Kallianpur, I. B. Moore, P. A. Seidl, S. J. Seestrom-Morris, D. B. Holtkamp, S. J. Greene, and W. B. Cottingame, Phys. Rev. C **24** 231 (1981).

[16]R. A. Eisenstein and G. A. Miller, Comput. Phys. Commun. **11**, 95 (1976).

[17]C. Gustaffson and E. Lambert, Ann. Phys. (N.Y.) **111**, 304 (1978).

[18]C. W. de Jager, H. de Vries, and C. de Vries, At. Data. Nucl. Data Tables **14**, 479 (1974).

[19]V. Gillet and N. Vinh Mau, Nucl. Phys. **54**, 321 (1964).